Oncogenic and Tumor-Suppressive Functions of the RNA Demethylase FTO

Hidde R. Zuidhof and Cornelis F. Calkhoven

ABSTRACT

The epitranscriptome represents the more than 140 types of chemically varying and reversable RNA modifications affecting RNA fate. Among these, the most relevant for this review are the mRNA modifications N^6-methyladenosine and N^6,2′-O-dimethyladenosine. Epitranscriptomic mRNA biology involves RNA methyltransferases (so-called "writers"), RNA demethylases ("erasers"), and RNA-binding proteins ("readers") that interact with methylation sites to determine the functional outcome of the modification. In this review, we discuss the role of a specific RNA demethylase encoded by the fat mass and obesity–associated gene (*FTO*) in cancer. FTO initially became known as the strongest genetic link for human obesity. Only in 2010, 16 years after its discovery, was its enzymatic function as a demethylase clarified, and only recently has its role in the development of cancer been revealed. FTO functions are challenging to study and interpret because of its genome-wide effects on transcript turnover and translation. We review the discovery of FTO and its enzymatic function, the tumor-promoting and suppressive roles of FTO in selected cancer types, and its potential as a therapeutic target.

Discovery of the *Fto* Gene

In an unsuccessful attempt to generate a transgenic mouse model overexpressing the human Harvey rat sarcoma viral oncogene homolog (*HRAS*), in 1994 a mutant was identified with syndactyly in both forelimbs that was named *Fused toes* (*Ft*; ref. 1). Homozygosity of the *Ft* mutation led to embryonic lethality around day 10 with embryos showing severely altered head morphology including missing large parts of the telencephalon and mesencephalon (1, 2). The mutation was later found to also cause a defect in establishing the left-right axis during embryonic development (3). Full mapping revealed a 1.6 Mb deletion on the long (q) arm of chromosome 8 covering genes currently known as Fused toes 1 (*Ft1*) or Akt-interacting protein (*Aktip*), retinitis pigmentosa GTPase regulator interacting protein 1 like (*Rpgrip1L*), Fat mass and obesity–associated (*Fto*) and three members of the Iroquois homeobox protein family *Irx3*, *Irx5*, and *Irx6* (4–6). Inactivation of mouse *Ft1/Aktip* results in telomeric defects associated with a progeroid phenotype (7, 8). Phenotypes of mice with a hypomorphic mutation in *Rpgrip1L* closely resemble those of *Ft*-mutant mice (9). Rpgrip1L has a critical function in the assembly of primary cilia and mutations in human RPGRIP1L cause the life-threatening diseases Joubert syndrome and Meckel syndrome (9–12). The *Irx* family members are conserved throughout insects, nematodes, and vertebrates and control tissue patterning in *Drosophila*, *Xenopus*, and mice (13, 14). In 1999, the cDNA of a 502 amino acid protein with no known homologs or conserved protein domains except for a bipartite nuclear localization signal was cloned (5). Southern blot analysis with probes spanning the cDNA confirmed total knockout of this gene in the *Ft* mutant and suggested a gene size of at least 250 kb, prompting the authors to name the gene Fatso (*Fto*; ref. 5).

The Genetic Link of *FTO* to Metabolism and Obesity

The distal region of mouse chromosome 8q covering the deletion in the *Ft* mutant is homologous to the long arm of human chromosome 16 (16q12-14; ref. 6). In 2007, four independent studies linked SNPs in *FTO* to obesity in humans (15–18). One of these studies focused on type 2 diabetes mellitus (T2DM) and identified several SNPs in the *FTO* gene to be significantly associated with T2DM in nearly 40,000 European adults (15). Obesity is a known risk factor for T2DM and the association between the SNPs and T2DM disappeared when correcting for body mass index (BMI), indicating the association of the SNPs with T2DM is mediated through BMI (15). Thereupon, "Fatso" was renamed to "Fat mass and obesity–associated," maintaining the *FTO* gene symbol. Although over 100 different loci have been found to robustly associate with BMI to date, the association with *FTO* remains the strongest of all genes in multiple ancestries (19). The first experimental link between FTO and obesity came with the discovery that whole-body knockout of *Fto* in mice leads to reduced bodyweight in both males and females, and significantly reduced weight gain in both sexes upon high-fat diet feeding (20). Offspring from heterozygous parents are born to Mendelian ratio and homozygous $Fto^{-/-}$ mice show normal development and weight at birth. However, postnatal survival of $Fto^{-/-}$ mice is decreased with 60% (20), which can be improved by reduction in litter size or postponed weaning, suggesting that the altered metabolism causes reduced survival after weaning. A knockin mouse model introducing the Fto^{I367F} mutant with reduced catalytic acitivty showed similar phenotypes as the $Fto^{-/-}$ model, albeit only in males and not in females (21). Ubiquitous overexpression of FTO in mice on the other hand leads to an increase in body weight and fat mass in both males and females, on a normal diet as well as on a high-fat diet (22). In humans a recessive loss-of-function mutation in *FTO* was discovered in an Arab family that leads to postnatal growth retardation, microcephaly, facial dimorphism, and functional brain deficits (23). All patients homozygous for the mutation died between 1 and 30 months of age, indicating additional functions of human

European Research Institute for the Biology of Ageing (ERIBA), University Medical Center Groningen, University of Groningen, Groningen, the Netherlands.

Note: Supplementary data for this article are available at Cancer Research Online (http://cancerres.aacrjournals.org/).

Corresponding Author: Cornelis F. Calkhoven, ERIBA, UMCG, Antonius Deusinglaan 1, Groningen 9713 AV, the Netherlands. Phone: 31-52-72-45-91; E-mail: c.f.calkhoven@umcg.nl

Cancer Res 2022;82:2201–12

doi: 10.1158/0008-5472.CAN-21-3710

FTO compared with murine *Fto* (23). In another human study, SNPs in *FTO* were associated with reduced brain volume in healthy elderly (24). Combined, these findings establish FTO as an important regulator of fat mass in murine models, with a strong genetic link to human obesity.

FTO Is an RNA-N^6-methyl Adenine Demethylase

At the time SNPs in the *FTO* gene were linked to obesity, the molecular function of FTO was unknown. Computational analysis revealed sequence similarity between FTO's N-terminus and members of the family of non-heme Fe(II)- and 2-oxoglutarate (also known as α-ketoglutarate)-dependent dioxygenases (2OGX; ref. 25). 2OGX proteins are found in species from mammals to green algae and are characterized by similar overall protein fold and the positioning of highly conserved residues involved in substrate binding and catalysis, despite a large overall divergence in primary amino acid sequence (26, 27). *In silico* predictions of FTO's protein structure closely resembled structures for the *E. coli* alpha-ketoglutarate–dependent dioxygenase AlkB, a member of the 2OGX family, despite a mere 17% sequence identity between the two (25). Studies using structural analysis and comparative analysis of enzymatic activities between FTO and other 2OGX proteins (25, 27–31) and enhanced UV cross-linking immunoprecipitation analysis altogether revealed that FTO enzymatic function is to demethylate N^6-methyladenosine (m^{6}A) residues in mRNA, small nuclear RNA (snRNA), small nucleolar RNAs (snoRNA) as well as of m1A in transfer RNA (**Fig. 1A**; refs. 32–34). m^{6}A modification of mRNAs are associated with various functions, often context specific, through regulation of mRNA fate and translation. A more elaborate description relevant for this review is found in the next section as well as we would like to refer other published reviews (35, 36).

m^{6}A modifications seem to accumulate near stop codons and in the 3′ UTR (untranslated region), are less frequent in the coding sequence, and are mostly depleted from the 5′ UTR (37–39). By genome-wide methylated RNA immunoprecipitation sequencing (MeRIP-seq) an m^{6}A-methylation consensus site was identified as RRACH (H = A,C,U and R = A/G; ref. 38). Yet, some studies have not found enrichment of RRACH sequence motifs for FTO in CLIP analyses (40, 41), or only found them upon exogenous FTO overexpression (42). Furthermore, FTO has a relatively low substrate affinity for m^{6}A-mRNA and the conversion of m^{6}A into A is relatively slow (32, 34, 43). Noteworthy here is that the catalyzation involves two steps of conversion of m^{6}A into hydroxymethyladenosine (hm^{6}A) and release of A and formaldehyde. FTO generates hm^{6}A as the major product, followed by a release of A and formaldehyde over longer times, which is in contrast to the ALKBH5 2OGX-protein that catalyzes conversion into A with concomitant release of formaldehyde (44, 45). Transcriptome-wide MeRIP-seq studies using an antibody recognizing methylated m^{6}A and cap-specific N6,2′-O-dimethyladenosine (m^{6}Am) revealed m^{6}Am as FTO responsive sites in addition to m^{6}A (**Fig. 1B**; refs. 39, 43, 46, 47). Subsequent biochemical experiments revealed the catalytic efficiency (k_{cat}/K_m) for FTO toward m^{6}Am to be around 100-fold higher than for m^{6}A (43). Depletion of FTO using siRNA from HEK293 cells resulted in increased methylation of cap-specific m^{6}Am but not m^{6}A as was analyzed by thin layer chromatography (43). The proposition that FTO does not affect m^{6}A in mRNA to a biologically meaningful extent has however been questioned by others in the field, and clashes with a substantial amount of literature. For example, increased mRNA-m^{6}A levels were found in brain tissue from *Fto* knockout mice (46), liver-specific FTO overexpression reduced mRNA-m^{6}A levels in mice (48) and knockdown of FTO increased mRNA m^{6}A levels in different acute myeloid leukemia (AML) cell lines (49, 50), Hep-G2 cells (51) and HeLa, HEK293T and 3T3-L1 cells (34). The ability of FTO to demethylate cap-specific m^{6}Am but also m^{6}A was additionally confirmed by mass spectrometry analysis of purified mRNA (34, 52). Furthermore, the metabolite NADP was shown to directly bind FTO and stimulates its m^{6}A demethylation activity to regulate adipogenesis (53). In addition, when FTO was overexpressed in rice and potato plants, m^{6}A levels of mRNA and nonribosomal RNA and gene expression were significantly affected, resulting in grain yield and increased biomass (54). Remarkably, both rice and potato do not contain an FTO or an m^{6}Am-methyltransferase homolog and have no m^{6}Am at their mRNA 5′-cap (54). For interpretation of the data, several issues have to be considered. Some of the aforementioned studies rely on semiquantitative mRNA dot blotting or m^{6}A mass spectrometry measurements to determine mRNA-m^{6}A levels, both of which are highly sensitive to the purity of input mRNA and can be affected by for example ribosomal RNA if sample preparation is suboptimal (55).

Furthermore, studies that rely on MeRIP-seq might not be as reliable as initially thought. Reanalysis of MeRIP-based studies revealed considerable interreplicate variation and poor reproducibility across studies due to noise and difficulties in separating underlying expression changes from changes in m^{6}A level (56). Additional more advanced techniques to quantify m^{6}A modification at specific sites transcriptome-wide have recently been developed and rely on mazF endonuclease that cleaves unmethylated ACA motifs, but leaves "m^{6}A-CA" motifs intact (MAZTER-seq/m^{6}A-REF-seq; refs. 57, 58). When mRNA isolated from HEK293T cells was treated *in vitro* with FTO, m^{6}A-REF-seq identified a significant decrease in m^{6}A levels (58). However, when FTO was either knocked out or overexpressed in human embryonic stem cells or HEK293T cells, no impact on m^{6}A levels was found in any condition with MAZTER-seq, in contrast to overexpression of ALKBH5 or knockout of METTL3 (57). It should be noted techniques based on mazF nuclease can by their nature only identify around 16% of mammalian m^{6}A sites, due to the requirement for the ACA motif and ACA-site spacing constraints (57), and therefore the technique would greatly benefit from the development of other/less context specific m^{6}A-sensitive nucleases.

Notably, *in vitro* studies identify cap-specific m^{6}Am as the most efficiently converted substrate in biochemical assays with purified components (34, 43, 52). Nonetheless, in mRNAs from different mammalian cell lines and human and mouse tissues including cortex, liver, heart, skin, adipose, neurons and digestive tissues, m^{6}A is on average 10- to 20-fold more abundant, with some AML cell lines having 30-fold more m^{6}A over cap-specific m^{6}Am (34, 50, 52, 59–62). This makes m^{6}A in mRNAs the numerically more turned-over modification *in vitro* and might explain why many studies show an increase in transcriptome wide m^{6}A levels upon FTO depletion, despite its preference for cap-specific m^{6}Am demethylation over m^{6}A in experiments with synthetic single-stranded RNA (ssRNA; refs. 34, 52). In addition, subcellular localization of FTO has been argued to differ between cell lines (34) or during the cell cycle (63) and thereby determine what substrates are most readily available (34).

Besides mRNAs, cap-associated m^{6}Am modification of Sm-class snRNAs are increased by a substantial 10- to 20-fold upon FTO depletion in mouse liver and HEK293 cells and their demethylation by FTO was demonstrated in biochemical assays and cells (64). This was further supported by development of a novel method to quantify m^{6}A modifications transcriptome-wide at specific sites (m^{6}ACE-seq). m^{6}ACE-seq makes use of cross-linking an m^{6}A-antibody (also

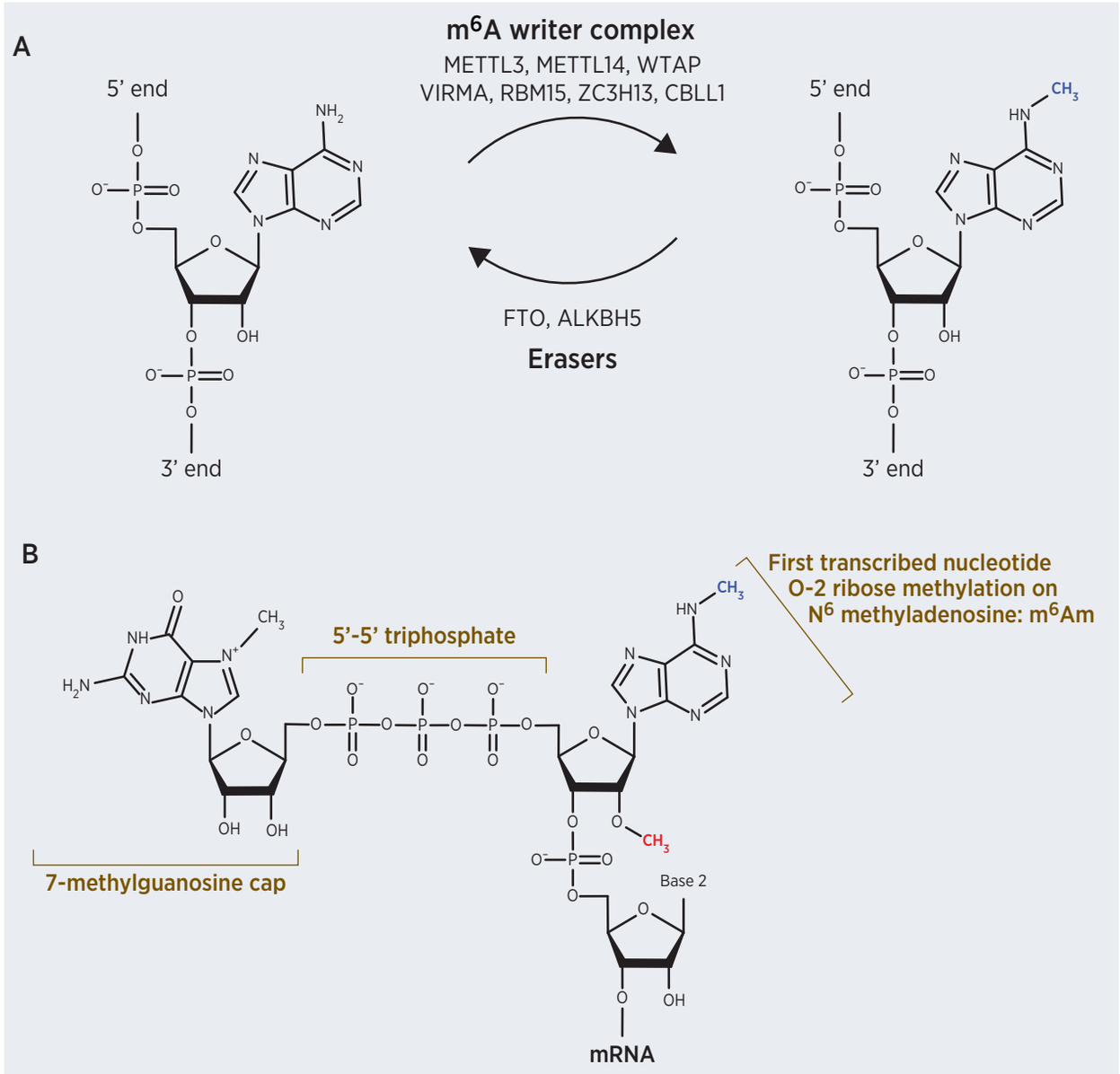

Figure 1.

Molecular structure of m^6A and m^6Am. **A,** Adenosine residues in RNA (left) can be methylated on the primary amine in position 6 to m^6A (right). The methyl group depicted in blue is added by a multiprotein methyltransferase writer complex consisting of the catalytic METTL3-METTL14 heterodimer and additional proteins such as Wilms' tumor 1–associating protein (WTAP), Vir like m^6A methyltransferase associated (VIRMA), RNA-binding motif protein 15 (RBM15), zinc finger CCCH-type containing 13 (ZC3H13), and Cbl proto-oncogene like 1 (CBLL1, also known as HAKAI). Demethylation of m^6A is catalyzed by two m^6A eraser proteins: FTO and AlkB homolog 5 (ALKBH5). **B,** Structure of a mammalian mRNA 7-methylguanosine cap linked to the first transcribed nucleotide via a 5′-5′ triphosphate bridge. Nucleotides at position +1 relative to the cap are often methylated on the 2′-hydroxyl of the ribose ring (red); for adenosine this results in 2′-O-methyladenosine (Am). Am at the +1 position can be further methylated on the primary amine (blue) to N^6,2-O-dimethyledenosine (m^6Am).

recognizing m^6Am) to m^6A, which blocks subsequent XRN1 exonuclease digestion and thereby marks sites of m^6A modification (65). Also in this study FTO depletion in HEK293T cells led to accumulation of m^6Am at the first nucleotide of several small RNAs (sRNA), snoRNAs, and Sm-class snRNAs, which was confirmed in biochemical assays, without significantly affecting mRNA m^6A levels (65). Hence m^6Am in snRNA was proposed to be the major target for FTO (64, 65).

Functional Consequences of m^6A Demethylation

To better understand the functional consequences of FTO's demethylation activities one has to consider the effects of mRNA (de)methylation. The (patho)physiologic effects of m^6A are mediated through m^6A-binding proteins. The most well studied of these so-called "m^6A-readers" are proteins that contain a YT521-B homology

(YTH) m^{6}A RNA-binding domain (66, 67). In humans five YTH domain containing proteins exist: YTH domain family member (YTHDF) 1, 2, and 3 that are cytosolic proteins with similar structure and YTH domain containing (YTHDC) 1 and 2 that show no homology apart from their YTH domains and are mostly nuclear (YTHDC1) or both cytoplasmic and nuclear (YTHDC2; reviewed in ref. 68). The study of YTH domain-containing proteins was intensified upon the discoveries that they bind to m^{6}A (38) and YTHDF2, similar to the yeast homolog of YTHDC1, promotes degradation of its target mRNA in mammalian cells (69). Some proteins lacking a YTH domain have also been proposed to bind m^{6}A directly, such as fragile X-mental retardation protein (FMRP), IGF 2 mRNA-binding proteins (IGF2BP) and subunits of eukaryotic initiation factor 3 (70–73). However, these proteins might interact with known m^{6}A-binding proteins, as has been shown for FMRP and YTHDF2, and further studies are required to confirm direct m^{6}A binding (74).

The most well-known downstream effect of m^{6}A modification is regulation of mRNA stability (reviewed in ref. 75). In particular under stress conditions, YTHDF proteins and their bound m^{6}A-modified mRNAs have been found to relocate to different phase separated compartments including P bodies (69, 76, 77), which are subcellular compartments where mRNAs are degraded through decapping and subsequent 5′ to 3′ exonucleolytic cleavage by XRN1 (78). In addition, direct interaction of YTHDF2 with the CCR4-NOT (carbon catabolite repression—negative on TATA-less) deadenylase complex (independent of P body factors) has been observed (79), which is notable given mRNA deadenylation is known to precede P body formation. A plausible model could be that YTHDF2 promotes recruitment of the multi complex CCR4-NOT to initiate transcript degradation by deadenylation with subsequent translocation to P bodies for decapping and further XRN1-mediated decay. Recently, an additional degradation pathway was proposed where YTHDF2 indirectly binds RNaseP/MRP to promote endonucleolytic cleavage of mRNA (80).

Nuclear export of mRNA is another process affected by m^{6}A modification. Nuclear YTHDC1 was shown to interact with serine and arginine rich splicing factor (SRSF) 3 and thereby promote export of m^{6}A-modified mRNAs via nuclear RNA export factor (NXF) 1 (81). NXF1 mediates the bulk of mRNA export, which requires interactions with the transcription export complex (TREX; reviewed in ref. 82). Components of the m^{6}A methyltransferase complex were shown to interact with subunits of the TREX complex and thereby stabilize YTHDC1 binding to mRNAs, which in turn stimulated mRNA export (83). Separate from NXF1, specific m^{6}A-modified mRNAs can be exported from the nucleus by exportin 1 (XPO1, also known as CRM1), the major mediator of protein nuclear export (72, 73, 84).

An m^{6}A-binding motif is not always required for interaction of a protein with m^{6}A-modified RNA. RNA structure mapping in RNAs from lymphoblastoid cells revealed that adjacent to RRACH m^{6}A consensus sites with increased paired conformation the RNA adopts an increased ssRNA conformation (85). These properties allow m^{6}A to execute a type of structural switch where a region of structured RNA is either stabilized or destabilized depending on the position of the modified residue. For example, in the MALAT1 lncRNA, m^{6}A modification destabilizes a hairpin structure and thereby exposes the single-stranded binding domain for binding by the RNA-binding protein (RBP) heterogeneous nuclear ribonuclear protein C (HNRNPC; refs. 86, 87). Global reduction of m^{6}A on mRNAs reduces HNRNPC binding at m^{6}A consensus sites transcriptome wide because of preferred duplex over ssRNA conformation (88). It will be important to assess the actual contribution of m^{6}A over a potential structural rearrangement following mRNA (de)methylation to fully understand RNA–protein interactions. Finally, it should be noted m^{6}A can also repel certain RBPs from their binding sites, for example, G3BP1 and LIN28A, although the physiologic relevance of this process remains unexplored (89, 90).

Functional Consequences of m^{6}Am Demethylation

Although the m^{6}Am modification has been known for quite some time, studying of how it affects mRNA fate was hampered due to a lack of identified writers, readers or erasers. The limited number of studies published so far delivered no consensus on how m^{6}Am affects mRNA on a transcriptional or translational level. For example, m^{6}Am was proposed to promote transcript stability by preventing decapping mRNA 2 (DCP2)-mediated mRNA decapping in HEK cells (43), where another study only observed increased transcript stability when in addition to m^{6}Am, m^{6}A was present (34).

With the identification of phosphorylated CTD interacting factor 1 (PCIF1) as a cap-specific methyltransferase (CAPAM), experimental assessment of this modification has become more accessible (91). Concerning mRNA stability, some studies show that PCIF1 knockout has no effect (91, 92) or only for mRNAs in the lower half of expression levels (93). Concerning mRNA translation, studies report an increase (91), no difference (93, 94) or a decrease (92) of translation efficiency upon m^{6}Am modification. Potential mechanisms are still obscure, and m^{6}Am modification did not affect binding of the eukaryotic initiation factor 4E (eIF4E) to the cap as the initiating step in mRNA translation (91, 95). Comparing transcript regulation in testes, brain, and spleen upon *Pcif1* knockout in mice, the sets of upregulated and downregulated genes showed hardly any overlap between the tissues (94), questioning a substantial global effect of m^{6}Am on transcript stability across tissues. Also, transcripts starting with an adenosine showed lower expression in *Pcif1* knockout mice compared with wild-type mice only in the testes and not in the brain or spleen (94). In a study using colorectal cancer stem cells (CSC) cytoplasmic mRNA-m^{6}Am was identified as FTO's main target (96). Upon FTO knockdown in these cells, *in vivo* tumorigenicity was increased along with m^{6}Am levels despite marginal effects on both transcriptome and translatome. Both of these phenotypes were completely reversed upon knockdown of PCIF1/CAPAM (96). A systematic study on the effect of the identity and methylation status of the first transcribed nucleotide on protein expression found large differences between the HeLa, MEF, and JAWS II (murine immature dendritic cell line) cells (95). m^{6}Am compared with A as first nucleotide was shown to have no (MEF) a small (HeLa) or a large (JAWS II) effect on the expression of a reporter protein (95). Mapping of m^{6}A and m^{6}Am in different human and mouse tissues and human cell lines additionally showed extensive tissue specificity, and although not in all tissues, m^{6}Am was in general negatively correlated with protein levels from the Human Proteome Map (97). Apart from mRNA regulation, m^{6}Am modifications in snRNAs are deposited by METTL4 (98, 99) and mice with *Mettl4* knockout display anatomic defects including craniofacial dysmorphism with incomplete penetrance (100).

FTO in Cancer

In the past decade, FTO emerged as a relevant factor in cancer development. Not surprising in light of the global effects of FTO m^{6}A (m)-mRNA demethylation a picture emerges of pleiotropic and context-depending functions of FTO ranging from stabilization of

oncogenic mRNAs, cancer-specific changes in cellular metabolism and tumor immune evasion. FTO expression and function has been linked to several cancer types (Supplementary Table S1). Compromising FTO function experimentally in cancer cells in most cases reduces oncogenic potential measured by cell proliferation and migration. Nonetheless, tumor-suppressive functions of FTO also have been reported. Often, the mechanisms by which FTO promotes or inhibits tumorigenesis are not clarified. Yet, in several cases, the involved oncogenic mechanisms have been revealed, which are discussed here. However, the data that suggest an oncogenic role of FTO are in contradiction with genome-wide screening approaches that have been used in recent years to determine gene essentiality and their effect on cancer growth, including over 1,000 cancer cell lines in the Cancer Dependency Map (DepMap; depmap.org). For example, in AML cell lines where growth effects were observed as discussed below (49, 50), no effects are seen in genome-wide screens (101, 102). These findings extend to the rest of the DepMap that overall indicate no requirement for FTO in cancer growth. Although of great value the DepMap dataset and related analysis have also important limitations. The DepMap addresses the genetic requirements for cancer cell proliferation and survival in cell culture, which greatly differs from *in vivo* tumorigenesis in patients or in animal models. To mention a few; use of (different) nutrient-enriched and growth factor–enriched growth media, a two-dimensional rather than a three-dimensional environment, and the presence of a physiologic microenvironment and associated functional immune system. Therefore, how FTO as a factor that does not appear to be essential for cancer cell growth in large-scale drug and genetic perturbation platforms is identified as an oncogene in so many other studies (Supplementary Table S1), is a matter of concern, yet needs to be scrutinized by further studies.

Oncogenic Activities of FTO

m^6A modification is associated with a lower mRNA stability. FTO expression has been found elevated in several cancers and FTO-mediated m^6A-mRNA demethylation is shown to stabilize mRNAs encoding oncogenic factors in several cases.

AML

A couple of publications describe various oncogenic roles of FTO in the development of AML. Analysis of microarray and transcriptome data revealed that FTO is highly expressed in AML with t(11q23)/MLL rearrangements, t(15;17)/PML-RARA, FLT3-ITD, and/or NPM1 mutations (49). Fusion proteins resulting from MLL rearrangements cause enhanced demethylation of CpG islands in the *FTO* locus, resulting in upregulation of *FTO* transcription. In an MLL-AF9 fusion model of leukemia induction [AF9 is a component of the super elongation complex (SEC; ref. 103)], the enhanced *Fto* expression accelerated leukemogenesis while *Fto* deficiency delays it. Taken together, the data from *in vitro* and *in vivo* experiments suggest that certain cancer cells become reliant on increased FTO expression. The high expression of FTO cause m^6A demethylation and degradation of a subset of transcripts, among them are ankyrin repeat and SOCS box containing 2 (ASB2) and retinoic receptor alpha (RARA) as key regulators of AML. Which m^6A reader proteins might be involved remained unclear as YTHDF1/2 knockdown did not affect the transcript stability (49). Subsequent studies discovered that for R-2-hydroxyglutarate (R-2HG)-sensitive subtypes of AML, R-2HG acts tumor suppressive by inhibiting FTO catalytic activity (50). R-2HG is produced by mutant isocitrate dehydrogenase 1 and 2 (IDH1/2), which are frequent somatic lesions found in glioma (~80%) and AML (10%–20%; refs. 104–106). Inhibition of FTO by R-2HG results in accumulation of m^6A on MYC transcripts, decreasing its stability and downregulation of oncogenic MYC functions. In addition, R-2HG caused downregulation of FTO by suppression of CCAAT/enhancer binding protein alpha (C/EBPα) through accumulation of m^6A on CEBPA-mRNAs and its destabilization. C/EBPα is one of the transcriptional activators of FTO. Here, data indicate that YTHDF2-dependent mechanisms are involved in the degradation of the mRNAs. Remarkably, cap-specific m^6Am levels were found to be very low in AML, challenging a pathophysiologic role for this modification in hematopoiesis and leukemia. In another study, metabolomics analysis showed that FTO inhibition by R-2HG attenuates glycolysis flux in AML cells through m^6A accumulation on lactate dehydrogenase B (LDHB) and phosphofructokinase platelet (PFKP) transcripts and degradation through binding to YTHDF2 (107). Combined, these data suggest AML cells with high FTO expression rely on FTO-mediated m^6A demethylation to degrade transcripts of tumor suppressors and promote stability of oncogenes like MYC (50) and metabolic regulators such as PFKP and LDHB (107), contributing to cell proliferation and a block in differentiation. AML subtypes with either low endogenous FTO or IDH mutation (R-2HG–sensitive subtypes) on the other hand have found other ways to activate protumorigenic pathways and remain refractory to FTO inhibition.

Glioma

In the same study addressing FTO inhibition in R-2HG–sensitive AML, R-2HG also was found to act tumor suppressive by inhibiting FTO in glioma cells through accumulation of m^6A on MYC transcripts and downregulation of MYC oncogenic functions (50). Gliomas are tumors arising from glial cells in the brain or spinal cord, among which, glioblastoma is the most well-known and deadly subtype (108). These heterogeneous tumors contain glioblastoma stem cells (GSC) that display increased radiotherapy and chemotherapy resistance (108). In primary GSC cultures, differentiation of GSCs to neurons and astrocytes was found accompanied by a substantial increase in accumulation of mRNA-m^6A (109). Reduction of m^6A levels by knockdown of methyltransferase (METTL)3 or METTL14 led to increased maintenance of stem cell properties, while overexpression of METTL3 had an opposite effect (109). Increasing m^6A levels in primary GSCs by treatment with the FTO inhibitor MA2 (ethyl ester form of meclofenamic acid) furthermore reduced tumor growth in xenograft experiments (109). Among other mRNAs, ADAM19-mRNA encoding a transmembrane metalloprotease that is overexpressed in glioblastoma and promotes cell growth and invasion was found to be destabilized by accumulation of m^6A upon FTO inhibition (109). In an unrelated study, a negative feedback loop of MYC and MAX interactor 1 (MXI1) mediated by miR-155/23a cluster was identified that affected proliferation of glioma cells (110). MXI1 inhibits the transcriptional activity of MYC by competitive binding to MAX, which is the heterodimerization partner of MYC in an active transcription-promoting complex (111). The study shows that FTO-dependent upregulation of MYC results in miR-155/23a–mediated suppression of MXI1 (110). In addition, treatment with FTO-inhibitor MA2 decreased MYC in glioma cells and led to reduced proliferation (110). Patients with glioma are often treated with the chemotherapeutic temozolomide, which has been shown to reduce MYC levels through increased activity TAp63, a repressor of MYC transcription (112). Treatment of glioma cell lines with both MA2 and temozolomide had a stronger effect on MYC and cell proliferation than either single treatment, although effects were additive at best (110).

Lung cancer

Around 80% of lung cancers can be classified as non–small cell lung cancer (NSCLC), of which, lung adenocarcinoma (LUAD) and lung squamous cell carcinoma (LUSC) are two major subtypes (113). The role of FTO in NSCLC remains poorly understood and while some find poorer patient survival in high FTO-expressing LUSC but not in LUAD (113), others found no differences in LUSC and rather an increase in survival in high FTO LUAD (114). Generally, however, FTO appears to promote growth of multiple NSCLC cell lines from both subtypes. Knockdown of *FTO* impaired proliferation and migration in various LUSC cell lines while overexpression of FTO but not a catalytically inactive FTO mutant led to opposite phenotypes (113). Mechanistically, FTO was shown to demethylate m^{6}A and thereby stabilize myeloid zinc finger 1 (MZF1)-mRNA (113), a factor shown to induce MYC transcription and thereby promote tumorigenesis in LUAD (115). Although this link was not investigated explicitly in the aforementioned study, ectopic MZF1 expression was sufficient to restore cell growth defects upon *FTO* knockdown (113). The positive effect of FTO on NSCLC growth was also found in mouse xenograft experiments using A549 human NSCLC cells with *FTO* knockdown, which exhibited reduced tumor growth compared with control cells (116). The study shows that ubiquitin-specific peptidase 7 (USP7)-mRNA becomes hypermethylated upon *FTO* knockdown with a concomitant decrease in its transcript levels (116). In addition, ectopic USP7 expression could rescue the growth defect induced by *FTO* knockdown by yet unclear downstream molecular mechanisms (116). It should be noted that in above-mentioned studies targets are selected based either on profiling of FTO targets in AML or on previously described relevance to lung cancer, precluding the unbiased identification of additional and/or lung cancer specific targets of FTO.

Breast cancer

Expression of the estrogen receptor [ER$^-$ (negative)/ER$^+$ (positive)], the progesterone receptor (PR$^{-/+}$) and amplification of the HER2 (HER2$^+$) serve as markers for the different subtypes of breast cancer, including triple-negative breast cancer (TNBC; ER$^-$, PR$^-$, HER2$^-$), luminal A (ER$^+$, PR$^{+/-}$, HER2$^-$), luminal B (ER$^+$, PR$^{+/-}$, HER2$^{+/-}$; HER2$^+$: ER$^-$, PR$^-$, HER2$^+$; ref. 117). In luminal A and TNBC cell lines, *FTO* knockdown both *in vitro* and *in vivo* increased apoptosis, reduced migratory capacity and reduced cell growth (118). The study revealed FTO demethylates the mRNA encoding BCL2 interacting protein (BNIP)3, a proapoptotic BCL2-family member, and BNIP3 protein levels are increased upon *FTO* knockdown through an unidentified, YTHDF2-independent mechanism (118). In a different study, FTO was shown to promote migration and invasion but not proliferation in HER2$^+$ cells (119). Focusing on miRNA regulation, increased miR181b-3p levels were observed upon *FTO* knockdown or treatment with FTO inhibitor MA2 and the ADP ribosylation factor like GTPase (ARL)5B was identified as a major target of miRNA miR-181b-3p (119). ARL5B is an ADP ribosylation factor-like (ARL) family member that regulates lysosome transport and has been implicated in the regulation of pancreatic cancer cell migration (120). Indeed, ARL5B modulation mimics or restores the FTO-induced migration phenotype in HER2$^+$ breast cancer cell lines (119). How miR-181b-3p levels are regulated by FTO remains unclear; although a substantial number of miRNAs was shown to contain m^{6}A, miR-181b-3p was not among them and FTO deficiency did not affect its transcript level in HEK cells (121).

FTO Regulation of Immune Surveillance

Tumor neoantigens generated by cancer cells provoke spontaneous immune response as well as they offer targets for immunotherapies. However, a sufficient and lasting anticancer immune response leading to complete tumor elimination is rare. Cancer cells may escape immune surveillance by mounting mechanisms of immune evasion. Evidence is mounting that the epitranscriptome is involved in immune evasion. It was shown that transcripts encoding lysosomal proteases accumulate m^{6}A and that subsequent binding of YTHDF1 enhances their translation in dendritic cells (122).The enhanced lysosomal degradation of engulfed neoantigens suppresses the cross-presentation of neoantigens by the dendritic cells to CD8$^+$ T cells as a mechanism of immune evasion. Consequently, *Ythdf1* deficiency in mice results in an elevated antigen-specific CD8$^+$ T-cell antitumor response (122). It should however be noted here the effect of YTHDF1–3 proteins on translation has been disputed and a redundant role in promoting degradation of m^{6}A-modified transcripts has been proposed (123, 124).

In a different study, bioinformatic analysis revealed that FTO exhibit the most significant negative association with cytotoxic T lymphocyte score in melanomas and other cancer types. This led to the suggestion that FTO acts as an immune inhibitory factor for tumor-infiltrating function of CD8$^+$ T cells (125). The study concludes that FTO promotes tumor immune evasion as an epitranscriptomic regulator of glucose metabolism through m^{6}A demethylation of transcripts encoding the transcription factors c-Jun, JunB, and C/EBPβ. The resulting enhanced expression of these factors transcriptionally activates downstream glycolytic genes. High consumption of glucose by tumor cells is known to restrict T cells metabolically. *Fto* knockdown in melanoma (B16-OVA) and lung cancer cell lines inoculated in immune proficient mice resulted in smaller tumor sizes while in immunedeficient mice inoculation showed no difference between wild-type and *Fto*-knockdown cells. In addition, a 2-fold increase in infiltration of tetramer$^+$ CD8$^+$ T cells was observed in *Fto*-knockdown versus wild-type tumors. Transcriptome analysis showed enhanced expression of cytokines and cytotoxic molecules upon *Fto* knockdown in T cells cocultured with *Fto*-knockdown tumor cells show a higher cytotoxic state. Moreover, similar to *Fto* knockdown, treatment with the FTO-inhibitor Dac51 resulted in accumulation of m^{6}A and reduction in expression of c-Jun, JunB, and C/EBPβ as well as an inhibition of glycolysis in patient-derived organoids. Further *in vivo* studies in mice showed that treatment with Dac51 increases T-cell infiltration of B16-OVA melanoma cells similarly to *Fto*-knockdown tumor cells. Moreover, Dac51 treatment was shown to synergize with anti-PD-L1 immune checkpoint blockade.

Tumor-Suppressive Activities of FTO

Notwithstanding the well-described oncogenic roles of FTO as discussed above several studies present strong cases of FTO in a tumor-suppressive role.

Ovarian cancer

In ovarian tumors and CSCs, FTO expression was found suppressed and associated with increased global m^{6}A RNA levels (126). Moreover, FTO overexpression inhibited CSC proliferation and tumor initiation capacity in cell culture and xenograft mouse models. Furthermore, expression of a mutant FTO lacking demethylase function was ineffective in altering stemness phenotypes. Transcriptome-wide RNA sequencing and m^{6}A mapping identified over 700 significantly deregulated transcripts as a consequence of m^{6}A modifications with pathways

related to mRNA transcription and splicing, stem cell signaling and DNA repair. As the most prominent FTO targets two phosphodiesterase genes (PDE4B and PDE1C) were selected, which regulate cAMP signaling as a key pathway in maintaining stemness. The authors claim to provide the first solid evidence that FTO function acts tumor-suppressive in certain cancer types or stages (126).

Colorectal cancer

In a recent study involving CSCs, the cap-specific m^6Am modification was identified as an epitranscriptomic mark for maintaining stem-cell phenotype of colon cancer cells (96). Knockdown of *FTO* in various experimental settings promotes CSC phenotypes, including initiation of tumor formation and resistance to chemotherapeutic drugs in mouse xenograft models. Analyses of tumor arrays revealed that although global FTO expression does not change in different colorectal stages, the subcellular localization of FTO changes from strictly nuclear to cytoplasmic in metastatic submucosal invasion. This may be related to altered function of FTO. However, the mechanisms involved in suppressing FTO functions is CSC remain obscure also because no large differences were found in transcriptome analysis and a translation assay by polysome mapping (96).

Hepatocellular carcinoma

Studies using hepatocellular carcinoma (HCC) cell lines initially suggested FTO as a protumorigenic factor. In mouse xenograft experiments using HepG2 cells, *FTO* deficiency led to a significantly lower tumor volume, possibly through demethylation and stabilization of pyruvate kinase M2 (PKM2) mRNA (127). In addition, knockdown of *FTO* in HepG2 cells reduced the expression of lipogenesis genes, resulting in deficiency of lipid accumulation and induction of cellular apoptosis, suggesting a role for FTO in cancer cell survival and hepatocellular metabolism (128). However, in a recent study using a mouse model with hepatic *Fto* deficiency (FTOL-KO), only minor systemic metabolic changes were found (129). Long-term treatment with diethylnitrosamine (DEN), which provokes HCC, produced fewer and smaller tumors in the *Fto*-proficient compared with *Fto*-deficient mice (129). The study proposes the involvement of Cullin 4A (Cul4a) as a member of E3 ubiquitin ligase complexes that regulate cell-cycle progression and DNA replication. In wild-type livers, short-term high-dose DEN treatment resulted in an increase in FTO expression and a decrease in Cul4a protein levels, whereas in *Fto*-deficient livers Cul4a expression is maintained (129). Although in *Fto*-deficient livers Cul4a-mRNA showed an increase in m^6A modification compared with wild-type livers upon DEN treatment, transcript levels remained unaffected. The authors therefore proposed that sustained translation of hypermethylated *Cul4a* induced the expression of its target genes such as cyclin E1 to promote HCC development (129). Lower FTO levels compared with surrounding healthy tissue were indeed observed for HCC in a limited number of patients (130). In further support of a tumor-suppressive role of FTO, low expression levels of FTO were found to be associated with poor prognosis and chemotherapy resistance in intrahepatic cholangiocarcinoma (cancer of the bile duct epithelial cells; ref. 131). Here, FTO expression promoted apoptosis and reduced cell growth and migration both *in vitro* and in mouse xenograft experiments (131).

Epithelial–Mesenchymal Transition–Mediated Tumor Progression

By analyzing multiple datasets on cancer, Jeschke and colleagues noted that FTO is downregulated in various epithelial tumors (132). Experiments in cell culture showed that FTO depletion in several breast and prostate cancer cell lines increased clonogenicity, invasiveness and migratory potential. Moreover *in vivo* xenotransplant experiments in mice showed increased tumor progression after FTO depletion as well as by inhibition of FTO with meclofenamic acid. Gene expression analysis revealed an activated epithelial–mesenchymal transition (EMT) program in *FTO* knockdown cancer cells and xenograft tumors, while in patient samples lower expression of FTO was significantly correlated with a high EMT signature. In particular, many mRNAs encoding factors in the Wingless (Wnt)-β-catenin signaling pathway showed increased m^6A deposition. In breast cancer cells, knockdown of *FTO* resulted in stabilization of the Wnt-ligand Wnt family member 54 (WNT5A) while at the same time destabilization of transcripts encoding casein kinase I subunits CSNK1D/G2 involved in β-catenin destruction, illustrating the diverse effects of m^6A modifications. Because FTO-low type epithelial tumors rely on Wnt signaling to activate EMT, treatment with the Wnt inhibitor iCRT3 reduced tumor clonogenicity and invasiveness of tumor cells specifically after FTO knockdown or tumor progression in xenotransplant mouse models. Note that the conclusions from the study described in this paragraph (132) contradict with the studies described above that infer an oncogenic role of FTO in breast cancer (118, 119).

Therapeutic Implications

Several small-molecule inhibitors for FTO with varying potency and specificity have been developed since its crystal structure was solved in 2010 (31). The first identified inhibitor, rhein, has a broad inhibitory effect on AlkB family proteins by competitive binding at the catalytic active site preventing binding of m^6A-mRNA (133). Despite the weak substrate specificity, allograft experiments in mice using 4T1 breast cancer cells demonstrated rhein treatment can reduce tumor growth albeit less efficiently than *Fto* knockdown (118).

As an 2OGX/AlkB family member, FTO requires bound Fe(II) and 2-oxoglutarate as cofactors for oxidative demethylation of m^6A (134). Many inhibitors for 2OGX proteins chelate the Fe(II) moiety, thereby preventing 2-OG and substrate binding, while others chemically mimic 2-OG (135). *In silico* docking and molecular modeling studies have been used to define a molecular blueprint for potential inhibitors or to further optimize low-affinity inhibitors. For example, compound 12 mimics 2-OG and protrudes into the nucleotide-binding site and was the first reported inhibitor with specificity for FTO over other AlkB family proteins (around 30-fold with an IC_{50} <1 μmol/L; ref. 136). The cell permeable ethyl ester of compound 12 was partially taken up and active in HeLa cells, resulting in a dose-dependent increase of m^6A in mRNA (136).

Meclofenamic acid (MA) is an FDA-approved NSAID that was also found to inhibit FTO, but not ALKBH5, with an IC_{50} of 7 μmol/L (137). Although this affinity is quite low, at high (80–120 μmol/L) concentrations the ethyl ester of MA (MA2) can increase mRNA m^6A levels in HeLa cells through FTO inhibition (137). MA2 treatment of glioblastoma stem cell lines at similar or slightly lower concentrations increased m^6A levels and inhibited cell growth both *in vitro* and in *in vivo* xenograft experiments (109). Although MA2 had to be delivered intratumorally, this provided another example of how small-molecule targeting of FTO can reduce cancer growth. On the basis of the crystal structure of the FTO/MA complex, MA was optimized *in silico* for improved biological activity and cellular uptake while retaining target specificity, resulting in FB23 and FB23-2 (138). FB23-2

showed an IC_{50} of 2.6 μmol/L toward FTO while resulting in moderate uptake in different AML cell lines, increased mRNA m^6A levels, growth inhibition, and a relatively high specificity exemplified by a large overlap in transcriptomes of cells treated with FB23-2 compared with genetic FTO depletion (138). FB23-2 was well tolerated *in vivo* and could effectively reduce growth of both patient-derived AML cells and AML cell lines in mouse xenograft experiments upon intraperitoneal injection (138). Next, FB23 and FB23-2 were further optimized, resulting in Dac51 used to study the role of FTO in immune surveillance as discussed in the paragraph above (125). Because MA-derived inhibitors showed specificity for FTO over ALKHB5, a molecular docking approach was used to predict the structure of compounds binding in the same pocket with preferable membrane permeability, hydrophilicity, and molecular weight (139). Using this approach FTO-02 and FTO-04 (IC_{50} = 2.2 and 3.4 μmol/L, respectively) were identified as novel FTO inhibitors (139). Although these compounds are yet to be tested *in vivo*, FTO-04 showed high selectivity for FTO over ALKBH5 and prevented formation of neutrospheres from patient-derived GSCs without affecting healthy controls, concomitant with an increase in mRNA m^6A levels in treated cells (139).

In a similar experimental approach, The NCI developmental therapeutics program library of around 260,000 compounds were virtually docked to FTO's catalytic center (140). Two compounds, CS1 (bisantrene) and CS2 (brequinar), were identified that inhibited AML cell growth with IC_{50} concentrations around 100 nmol/L in multiple cell lines; considerably lower than the concentration of FB23-2 needed in the same cell lines (140). Both compounds substantially prolonged survival by inhibiting AML progression in patient-derived xenograft (PDX) models of AML, and at the same concentration CS1/2 were more effective than FB23-2 (140). As both compounds were also tolerated in mice at four times the concentration used for treatment in the PDX model (140), they are good candidates for bioavailability and efficacy studies for different cancer types that would benefit from FTO inhibition.

Yet another promising starting point for FTO inhibition might be entacapone, an FDA-approved inhibitor of catechol-*O*-methyltransferase canonically used as adjunctive treatment for Parkinson disease. In an effort to obtain FTO inhibitors for treatment of metabolic disease, FDA-approved drugs were screened for virtual molecular docking to FTO (51). On the basis of this screening approach, entacapone was identified and biochemically verified to bind FTO and inhibit its m^6A demethylase activity *in vitro* (IC_{50} = 3.5 μmol/L) and in mouse liver upon addition of entacapone to the diet (51). Although the chemical structure is distinct from MA-based inhibitors, entacapone displayed good specificity for FTO over other dioxygenases and did not affect DNA methylation or histone methylation patterns in Hep-G2 cells (51).

Taken together, structure-based design and virtual screening approaches have led to the development of a series of small-molecule FTO inhibitors. With multiple candidates showing biological activity against and specificity for FTO, future efforts towards improving bioavailability and pharmacokinetics might yield valuable FTO inhibitors for treatment of multiple diseases including cancer.

Discussion and Perspectives

It has become clear that m^6A and cap-specific m^6Am modifications on mRNAs and mRNA demethylation by FTO play important roles in posttranscriptional regulation of gene expression. The presence of m^6A can affect processes such as mRNA splicing, nuclear export, translation and stability by facilitating or preventing interaction with various RBPs. m^6A-induced binding by RBPs can either involve dedicated m^6A-recognizing proteins or be induced by changes in RNA folding facilitating binding of other RBPs. Cellular RNA is in constant and complex interaction with various RBPs throughout every stage of its life cycle, and it is therefore not surprising that perturbation of the demethylase function of FTO affects many steps in the mRNA processing and translation. The contribution of FTO to mRNA m^6A demethylation is however not uncontroversial and pinpointing downstream targets and reliably quantifying their m^6A level has often been difficult. The advent of transcriptome-wide quantitative methods to detect m^6A such as MAZTER-seq (57) and m^6ACE-seq (65) will improve the assessment of m^6A RNA deposition in response to various cellular perturbations, and proposed alterations in m^6A level should be confirmed by these transcript-specific quantitative methods (141, 142). In contrast to m^6A, the function of cap-specific m^6Am in regulating mRNA fate and cellular (patho)physiology is still poorly understood. The recent discoveries of PCIF1/CAPAM as a m^6Am writer (91) and FTO as the factor adjusting m^6Am levels required for inducing a CSC phenotype in colorectal cancer (96) is likely the first of further discoveries of m^6Am functionality. Similarly, the identification of snRNA m^6Am demethylation by FTO (64) provides a new avenue of research to be explored, which is facilitated by discovery of the snRNA m^6Am methyltransferase METTL4 (98, 99). Because the methyltransferases for m^6A in mRNA and m^6Am in mRNA as well as in snRNA have now been identified, this allows validation m^6A or m^6Am as FTO substrates by investigating the phenotypes of cells lacking the corresponding methyltransferase.

Subcellular compartmentalization of FTO may be different between cell types (34) and might be dynamically regulated in the cell cycle (63) or by external stimuli (143), which has to be taken into account as it directly influences substrate availability. In patients with colorectal cancer, for example, FTO was mainly nuclear in precursor lesions and healthy adjacent tissue but also found in the cytoplasm of more advanced stage colorectal cancer (96). Yet, care should be taken relying solely on antibody staining because some have been shown to cause artifactual staining and therefore knockout strategies should be used for validation (65). How FTO recognizes its targets remains another open question in the field because RNA-interaction studies identified no clear consensus binding site. In addition, our knowledge of FTO binding partners and how they might affect demethylation activity or substrate specificity is limited (144). In general, increased expression of FTO leads to reduced mRNA m^6A content, which in turn stabilizes transcripts by preventing degradation through canonical RNA degradation pathways facilitated by m^6A-binding proteins such as YTHDF2. However, one cannot rely on these general pathways to hold up in all tissue types or disease states. This is exemplified in AML where FTO-mediated demethylation of m^6A in 5′ terminal and internal exons led to stabilization of MYC-mRNA, while METTL14 silencing reduced m^6A in the MYC 3′ terminal exon, leading to transcript destabilization (50, 145). In addition, both oncogenic and tumor suppressive roles for FTO in the same tissue have been described in, for example, liver, kidney, and colorectal cancer. As the control of mRNA fate is largely dictated by interaction with different RBPs, identifying the landscape of RNA-protein interactions upon FTO modulation will undoubtedly shed light on the different roles of FTO in different cancer (sub) types. Expression patterns of RBPs differ between tissues and might

explain why some of FTO's effects are common among different cell types while other are restricted to a specific (potentially malignant) state of a particular tissue. Protumorigenic roles of FTO are now apparent in different cancer (sub)types and targeted pharmacologic inhibition of FTO led to reduced tumor growth in preclinical models of AML and glioma *in vivo* (49, 50, 107). In combination, a better understanding of the molecular processes downstream of FTO-mediated RNA demethylation and continued development of targeted therapies aimed at inhibiting FTO might prove a powerful strategy to combat certain cancers.

Authors' Disclosures

C.F. Calkhoven reports grants from KWF during the conduct of the study. No disclosures were reported by the other author.

Acknowledgments

H.R. Zuidhof was supported by the Dutch Cancer Society (KWF # 10080) through a grant to C.F. Calkhoven.

Received November 12, 2021; revised February 4, 2022; accepted March 16, 2022; published first March 18, 2022.

References

1. van der Hoeven F, Schimmang T, Volkmann A, Mattei MG, Kyewski B, Ruther U. Programmed cell death is affected in the novel mouse mutant Fused toes (Ft). Development 1994;120:2601–7.
2. Anselme I, Laclef C, Lanaud M, Ruther U, Schneider-Maunoury S. Defects in brain patterning and head morphogenesis in the mouse mutant Fused toes. Dev Biol 2007;304:208–20.
3. Heymer J, Kuehn M, Ruther U. The expression pattern of nodal and lefty in the mouse mutant Ft suggests a function in the establishment of handedness. Mech Dev 1997;66:5–11.
4. Lesche R, Peetz A, van der Hoeven F, Ruther U. Ft1, a novel gene related to ubiquitin-conjugating enzymes, is deleted in the Fused toes mouse mutation. Mamm Genome 1997;8:879–83.
5. Peters T, Ausmeier K, Ruther U. Cloning of Fatso (Fto), a novel gene deleted by the Fused toes (Ft) mouse mutation. Mamm Genome 1999;10:983–6.
6. Peters T, Ausmeier K, Dildrop R, Ruther U. The mouse Fused toes (Ft) mutation is the result of a 1.6-Mb deletion including the entire Iroquois B gene cluster. Mamm Genome 2002;13:186–8.
7. Cenci G, Ciapponi L, Marzullo M, Raffa GD, Morciano P, Raimondo D, et al. The analysis of pendolino (peo) mutants reveals differences in the fusigenic potential among drosophila telomeres. PLoS Genet 2015;11:e1005260.
8. La Torre M, Merigliano C, Burla R, Mottini C, Zanetti G, Del Giudice S, et al. Mice with reduced expression of the telomere-associated protein Ft1 develop p53-sensitive progeroid traits. Aging Cell 2018;17:e12730.
9. Vierkotten J, Dildrop R, Peters T, Wang B, Ruther U. Ftm is a novel basal body protein of cilia involved in Shh signalling. Development 2007;134:2569–77.
10. Wiegering A, Dildrop R, Kalfhues L, Spychala A, Kuschel S, Lier JM, et al. Cell type-specific regulation of ciliary transition zone assembly in vertebrates. EMBO J 2018;37:e97791.
11. Arts HH, Doherty D, van Beersum SE, Parisi MA, Letteboer SJ, Gorden NT, et al. Mutations in the gene encoding the basal body protein RPGRIP1L, a nephrocystin-4 interactor, cause Joubert syndrome. Nat Genet 2007;39:882–8.
12. Delous M, Baala L, Salomon R, Laclef C, Vierkotten J, Tory K, et al. The ciliary gene RPGRIP1L is mutated in cerebello-oculo-renal syndrome (Joubert syndrome type B) and Meckel syndrome. Nat Genet 2007;39:875–81.
13. Hu W, Xin Y, Zhang L, Hu J, Sun Y, Zhao Y. Iroquois Homeodomain transcription factors in ventricular conduction system and arrhythmia. Int J Med Sci 2018;15:808–15.
14. Cavodeassi F, Modolell J, Gomez-Skarmeta JL. The Iroquois family of genes: from body building to neural patterning. Development 2001;128:2847–55.
15. Frayling TM, Timpson NJ, Weedon MN, Zeggini E, Freathy RM, Lindgren CM, et al. A common variant in the FTO gene is associated with body mass index and predisposes to childhood and adult obesity. Science 2007;316:889–94.
16. Dina C, Meyre D, Gallina S, Durand E, Korner A, Jacobson P, et al. Variation in FTO contributes to childhood obesity and severe adult obesity. Nat Genet 2007;39:724–6.
17. Scuteri A, Sanna S, Chen WM, Uda M, Albai G, Strait J, et al. Genome-wide association scan shows genetic variants in the FTO gene are associated with obesity-related traits. PLoS Genet 2007;3:e115.
18. Hinney A, Nguyen TT, Scherag A, Friedel S, Bronner G, Muller TD, et al. Genome wide association (GWA) study for early onset extreme obesity supports the role of fat mass and obesity associated gene (FTO) variants. PLoS One 2007;2:e1361.
19. Goodarzi MO. Genetics of obesity: what genetic association studies have taught us about the biology of obesity and its complications. Lancet Diabetes Endocrinol 2018;6:223–36.
20. Fischer J, Koch L, Emmerling C, Vierkotten J, Peters T, Bruning JC, et al. Inactivation of the Fto gene protects from obesity. Nature 2009;458:894–8.
21. Church C, Lee S, Bagg EA, McTaggart JS, Deacon R, Gerken T, et al. A mouse model for the metabolic effects of the human fat mass and obesity associated FTO gene. PLoS Genet 2009;5:e1000599.
22. Church C, Moir L, McMurray F, Girard C, Banks GT, Teboul L, et al. Overexpression of Fto leads to increased food intake and results in obesity. Nat Genet 2010;42:1086–92.
23. Boissel S, Reish O, Proulx K, Kawagoe-Takaki H, Sedgwick B, Yeo GS, et al. Loss-of-function mutation in the dioxygenase-encoding FTO gene causes severe growth retardation and multiple malformations. Am J Hum Genet 2009;85:106–11.
24. Ho AJ, Stein JL, Hua X, Lee S, Hibar DP, Leow AD, et al. A commonly carried allele of the obesity-related FTO gene is associated with reduced brain volume in the healthy elderly. Proc Natl Acad Sci U S A 2010;107:8404–9.
25. Sanchez-Pulido L, Andrade-Navarro MA. The FTO (fat mass and obesity associated) gene codes for a novel member of the non-heme dioxygenase superfamily. BMC Biochem 2007;8:23.
26. Aravind L, Koonin EV. The DNA-repair protein AlkB, EGL-9, and leprecan define new families of 2-oxoglutarate- and iron-dependent dioxygenases. Genome Biol 2001;2:RESEARCH0007.
27. Gerken T, Girard CA, Tung YC, Webby CJ, Saudek V, Hewitson KS, et al. The obesity-associated FTO gene encodes a 2-oxoglutarate-dependent nucleic acid demethylase. Science 2007;318:1469–72.
28. Jia G, Yang CG, Yang S, Jian X, Yi C, Zhou Z, et al. Oxidative demethylation of 3-methylthymine and 3-methyluracil in single-stranded DNA and RNA by mouse and human FTO. FEBS Lett 2008;582:3313–9.
29. Lee DH, Jin SG, Cai S, Chen Y, Pfeifer GP, O'Connor TR. Repair of methylation damage in DNA and RNA by mammalian AlkB homologues. J Biol Chem 2005;280:39448–59.
30. Yu B, Edstrom WC, Benach J, Hamuro Y, Weber PC, Gibney BR, et al. Crystal structures of catalytic complexes of the oxidative DNA/RNA repair enzyme AlkB. Nature 2006;439:879–84.
31. Han Z, Niu T, Chang J, Lei X, Zhao M, Wang Q, et al. Crystal structure of the FTO protein reveals basis for its substrate specificity. Nature 2010;464:1205–9.
32. Jia G, Fu Y, Zhao X, Dai Q, Zheng G, Yang Y, et al. N6-methyladenosine in nuclear RNA is a major substrate of the obesity-associated FTO. Nat Chem Biol 2011;7:885–7.
33. Van Nostrand EL, Pratt GA, Shishkin AA, Gelboin-Burkhart C, Fang MY, Sundararaman B, et al. Robust transcriptome-wide discovery of RNA-binding protein binding sites with enhanced CLIP (eCLIP). Nat Methods 2016;13:508–14.
34. Wei J, Liu F, Lu Z, Fei Q, Ai Y, He PC, et al. Differential m(6)A, m(6)Am, and m(1)A demethylation mediated by FTO in the cell nucleus and cytoplasm. Mol Cell 2018;71:973–85.
35. Frye M, Harada BT, Behm M, He C. RNA modifications modulate gene expression during development. Science 2018;361:1346–9.
36. Shi H, Wei J, He C. Where, when, and how: context-dependent functions of RNA methylation writers, peaders, and erasers. Mol Cell 2019;74:640–50.
37. Meyer KD, Saletore Y, Zumbo P, Elemento O, Mason CE, Jaffrey SR. Comprehensive analysis of mRNA methylation reveals enrichment in 3' UTRs and near stop codons. Cell 2012;149:1635–46.
38. Dominissini D, Moshitch-Moshkovitz S, Schwartz S, Salmon-Divon M, Ungar L, Osenberg S, et al. Topology of the human and mouse m6A RNA methylomes revealed by m6A-seq. Nature 2012;485:201–6.

39. Linder B, Grozhik AV, Olarerin-George AO, Meydan C, Mason CE, Jaffrey SR. Single-nucleotide-resolution mapping of m6A and m6Am throughout the transcriptome. Nat Methods 2015;12:767–72.
40. Zou S, Toh JDW, Wong KHQ, Gao Y-G, Hong W, Woon ECY. N6-Methyladenosine: a conformational marker that regulates the substrate specificity of human demethylases FTO and ALKBH5. Sci Rep 2016;6:25677.
41. Bartosovic M, Molares HC, Gregorova P, Hrossova D, Kudla G, Vanacova S. N6-methyladenosine demethylase FTO targets pre-mRNAs and regulates alternative splicing and 3'-end processing. Nucleic Acids Res 2017;45: 11356–70.
42. Li Y, Wu K, Quan W, Yu L, Chen S, Cheng C, et al. The dynamics of FTO binding and demethylation from the m6A motifs. RNA Biol 2019;16: 1179–89.
43. Mauer J, Luo X, Blanjoie A, Jiao X, Grozhik AV, Patil DP, et al. Reversible methylation of m(6)Am in the 5' cap controls mRNA stability. Nature 2017;541: 371–5.
44. Toh JDW, Crossley SWM, Bruemmer KJ, Ge EJ, He D, Iovan DA, et al. Distinct RNA N-demethylation pathways catalyzed by nonheme iron ALKBH5 and FTO enzymes enable regulation of formaldehyde release rates. Proc Natl Acad Sci U S A 2020;117:25284–92.
45. Fu Y, Jia G, Pang X, Wang RN, Wang X, Li CJ, et al. FTO-mediated formation of N6-hydroxymethyladenosine and N6-formyladenosine in mammalian RNA. Nat Commun 2013;4:1798.
46. Hess ME, Hess S, Meyer KD, Verhagen LA, Koch L, Bronneke HS, et al. The fat mass and obesity associated gene (Fto) regulates activity of the dopaminergic midbrain circuitry. Nat Neurosci 2013;16:1042–8.
47. Fu Y. Dynamic regulation of RNA modifications by AlkB family dioxygenases: The University of Chicago; 2012.
48. Zhou J, Wan J, Shu XE, Mao Y, Liu XM, Yuan X, et al. N(6)-methyladenosine guides mRNA alternative translation during integrated stress response. Mol Cell 2018;69:636–47.
49. Li Z, Weng H, Su R, Weng X, Zuo Z, Li C, et al. FTO plays an oncogenic role in acute myeloid leukemia as a N(6)-methyladenosine RNA demethylase. Cancer Cell 2017;31:127–41.
50. Su R, Dong L, Li C, Nachtergaele S, Wunderlich M, Qing Y, et al. R-2HG exhibits anti-tumor activity by targeting FTO/m(6)A/MYC/CEBPA signaling. Cell 2018;172:90–105.
51. Peng S, Xiao W, Ju D, Sun B, Hou N, Liu Q, et al. Identification of entacapone as a chemical inhibitor of FTO mediating metabolic regulation through FOXO1. Sci Transl Med 2019;11:eaau7116.
52. Zhang X, Wei LH, Wang Y, Xiao Y, Liu J, Zhang W, et al. Structural insights into FTO's catalytic mechanism for the demethylation of multiple RNA substrates. Proc Natl Acad Sci U S A 2019;116:2919–24.
53. Wang L, Song C, Wang N, Li S, Liu Q, Sun Z, et al. NADP modulates RNA m(6) A methylation and adipogenesis via enhancing FTO activity. Nat Chem Biol 2020;16:1394–402.
54. Yu Q, Liu S, Yu L, Xiao Y, Zhang S, Wang X, et al. RNA demethylation increases the yield and biomass of rice and potato plants in field trials. Nat Biotechnol 2021;39:1581–8.
55. Legrand C, Tuorto F, Hartmann M, Liebers R, Jacob D, Helm M, et al. Statistically robust methylation calling for whole-transcriptome bisulfite sequencing reveals distinct methylation patterns for mouse RNAs. Genome Res 2017;27:1589–96.
56. McIntyre ABR, Gokhale NS, Cerchietti L, Jaffrey SR, Horner SM, Mason CE. Limits in the detection of m6A changes using MeRIP/m6A-seq. Sci Rep 2020; 10:6590.
57. Garcia-Campos MA, Edelheit S, Toth U, Safra M, Shachar R, Viukov S, et al. Deciphering the "m6A Code" via antibody-independent quantitative profiling. Cell 2019;178:731–47.
58. Zhang Z, Chen L-Q, Zhao Y-L, Yang C-G, Roundtree IA, Zhang Z, et al. Single-base mapping of m6A by an antibody-independent method. Sci Adv 2019;5: eaax0250.
59. Wei C, Gershowitz A, Moss B. N6, O2'-dimethyladenosine a novel methylated ribonucleoside next to the 5' terminal of animal cell and virus mRNAs. Nature 1975;257:251–3.
60. Wei CM, Gershowitz A, Moss B. Methylated nucleotides block 5' terminus of HeLa cell messenger RNA. Cell 1975;4:379–86.
61. Engel M, Eggert C, Kaplick PM, Eder M, Röh S, Tietze L, et al. The role of m6A/m-RNA methylation in stress response regulation. Neuron 2018;99: 389–403.
62. Liu J, Li K, Cai J, Zhang M, Zhang X, Xiong X, et al. Landscape and regulation of m6A and m6Am methylome across human and mouse tissues. Mol Cell 2020; 77:426–40.
63. Hirayama M, Wei FY, Chujo T, Oki S, Yakita M, Kobayashi D, et al. FTO demethylates cyclin D1 mRNA and controls cell-cycle progression. Cell Rep 2020;31:107464.
64. Mauer J, Sindelar M, Despic V, Guez T, Hawley BR, Vasseur JJ, et al. FTO controls reversible m(6)Am RNA methylation during snRNA biogenesis. Nat Chem Biol 2019;15:340–7.
65. Koh CWQ, Goh YT, Goh WSS. Atlas of quantitative single-base-resolution N (6)-methyl-adenine methylomes. Nat Commun 2019;10:5636.
66. Imai Y, Matsuo N, Ogawa S, Tohyama M, Takagi T. Cloning of a gene, YT521, for a novel RNA splicing-related protein induced by hypoxia/reoxygenation. Brain Res Mol Brain Res 1998;53:33–40.
67. Stoilov P, Rafalska I, Stamm S. YTH: a new domain in nuclear proteins. Trends Biochem Sci 2002;27:495–7.
68. Patil DP, Pickering BF, Jaffrey SR. Reading m6A in the transcriptome: m6A-binding proteins. Trends Cell Biol 2018;28:113–27.
69. Wang X, Lu Z, Gomez A, Hon GC, Yue Y, Han D, et al. N6-methyladenosine-dependent regulation of messenger RNA stability. Nature 2014;505:117–20.
70. Meyer KD, Patil DP, Zhou J, Zinoviev A, Skabkin MA, Elemento O, et al. 5' UTR m(6)A promotes cap-independent translation. Cell 2015;163:999–1010.
71. Huang H, Weng H, Sun W, Qin X, Shi H, Wu H, et al. Recognition of RNA N (6)-methyladenosine by IGF2BP proteins enhances mRNA stability and translation. Nat Cell Biol 2018;20:285–95.
72. Hsu PJ, Shi H, Zhu AC, Lu Z, Miller N, Edens BM, et al. The RNA-binding protein FMRP facilitates the nuclear export of N (6)-methyladenosine-containing mRNAs. J Biol Chem 2019;294:19889–95.
73. Edens BM, Vissers C, Su J, Arumugam S, Xu Z, Shi H, et al. FMRP modulates neural differentiation through m(6)A-dependent mRNA nuclear export. Cell Rep 2019;28:845–54.
74. Zhang F, Kang Y, Wang M, Li Y, Xu T, Yang W, et al. Fragile X mental retardation protein modulates the stability of its m6A-marked messenger RNA targets. Hum Mol Genet 2018;27:3936–50.
75. Lee Y, Choe J, Park OH, Kim YK. Molecular mechanisms driving mRNA degradation by m6A modification. Trends Genet 2020;36:177–88.
76. Anders M, Chelysheva I, Goebel I, Trenkner T, Zhou J, Mao Y, et al. Dynamic m (6)A methylation facilitates mRNA triaging to stress granules. Life Sci Alliance 2018;1:e201800113.
77. Ries RJ, Zaccara S, Klein P, Olarerin-George A, Namkoong S, Pickering BF, et al. m6A enhances the phase separation potential of mRNA. 2019;571:424–8.
78. Sheth U, Parker R. Decapping and decay of messenger RNA occur in cytoplasmic processing bodies. Science 2003;300:805–8.
79. Du H, Zhao Y, He J, Zhang Y, Xi H, Liu M, et al. YTHDF2 destabilizes m(6)A-containing RNA through direct recruitment of the CCR4-NOT deadenylase complex. Nat Commun 2016;7:12626.
80. Park OH, Ha H, Lee Y, Boo SH, Kwon DH, Song HK, et al. Endoribonucleolytic cleavage of m(6)A-containing RNAs by RNase P/MRP complex. Mol Cell 2019; 74:494–507.
81. Roundtree IA, Luo GZ, Zhang Z, Wang X, Zhou T, Cui Y, et al. YTHDC1 mediates nuclear export of N(6)-methyladenosine methylated mRNAs. Elife 2017;6:e31311.
82. Delaleau M, Borden KL. Multiple export mechanisms for mRNAs. Cells 2015;4: 452–73.
83. Lesbirel S, Viphakone N, Parker M, Parker J, Heath C, Sudbery I, et al. The m(6) A-methylase complex recruits TREX and regulates mRNA export. Sci Rep 2018; 8:13827.
84. Hutten S, Kehlenbach RH. CRM1-mediated nuclear export: to the pore and beyond. Trends Cell Biol 2007;17:193–201.
85. Roost C, Lynch SR, Batista PJ, Qu K, Chang HY, Kool ET. Structure and thermodynamics of N6-methyladenosine in RNA: a spring-loaded base modification. J Am Chem Soc 2015;137:2107–15.
86. Liu N, Dai Q, Zheng G, He C, Parisien M, Pan T. N(6)-methyladenosine-dependent RNA structural switches regulate RNA-protein interactions. Nature 2015;518:560–4.
87. Zhou KI, Parisien M, Dai Q, Liu N, Diatchenko L, Sachleben JR, et al. N(6)-methyladenosine modification in a long noncoding RNA hairpin predisposes its conformation to protein binding. J Mol Biol 2016;428:822–33.
88. Spitale RC, Flynn RA, Zhang QC, Crisalli P, Lee B, Jung JW, et al. Structural imprints *in vivo* decode RNA regulatory mechanisms. Nature 2015;519:486–90.

89. Sun L, Fazal FM, Li P, Broughton JP, Lee B, Tang L, et al. RNA structure maps across mammalian cellular compartments. Nat Struct Mol Biol 2019; 26:322–30.
90. Edupuganti RR, Geiger S, Lindeboom RGH, Shi H, Hsu PJ, Lu Z, et al. N(6)-methyladenosine (m(6)A) recruits and repels proteins to regulate mRNA homeostasis. Nat Struct Mol Biol 2017;24:870–8.
91. Akichika S, Hirano S, Shichino Y, Suzuki T, Nishimasu H, Ishitani R, et al. Cap-specific terminal N (6)-methylation of RNA by an RNA polymerase II-associated methyltransferase. Science 2019;363:eaav0080.
92. Sendinc E, Valle-Garcia D, Dhall A, Chen H, Henriques T, Navarrete-Perea J, et al. PCIF1 catalyzes m6Am mRNA methylation to regulate gene expression. Mol Cell 2019;75:620–30.
93. Boulias K, Toczydlowska-Socha D, Hawley BR, Liberman N, Takashima K, Zaccara S, et al. Identification of the m(6)Am methyltransferase PCIF1 reveals the location and functions of m(6)Am in the transcriptome. Mol Cell 2019;75: 631–43.
94. Pandey RR, Delfino E, Homolka D, Roithova A, Chen KM, Li L, et al. The mammalian cap-specific m(6)Am RNA methyltransferase PCIF1 regulates transcript levels in mouse tissues. Cell Rep 2020;32:108038.
95. Sikorski PJ, Warminski M, Kubacka D, Ratajczak T, Nowis D, Kowalska J, et al. The identity and methylation status of the first transcribed nucleotide in eukaryotic mRNA 5' cap modulates protein expression in living cells. Nucleic Acids Res 2020;48:1607–26.
96. Relier S, Ripoll J, Guillorit H, Amalric A, Achour C, Boissiere F, et al. FTO-mediated cytoplasmic m(6)Am demethylation adjusts stem-like properties in colorectal cancer cell. Nat Commun 2021;12:1716.
97. Liu J, Li K, Cai J, Zhang M, Zhang X, Xiong X, et al. Landscape and regulation of m(6)A and m(6)Am methylome across human and mouse tissues. Mol Cell 2020;77:426–40.
98. Chen H, Gu L, Orellana EA, Wang Y, Guo J, Liu Q, et al. METTL4 is an snRNA m6Am methyltransferase that regulates RNA splicing. Cell Res 2020;30:544–7.
99. Goh YT, Koh Casslynn WQ, Sim DY, Roca X, Goh WSS. METTL4 catalyzes m6Am methylation in U2 snRNA to regulate pre-mRNA splicing. Nucleic Acids Res 2020;48:9250–61.
100. Kweon S-M, Chen Y, Moon E, Kvederaviciutė K, Klimasauskas S, Feldman DE. An adversarial DNA N6-methyladenine-sensor network preserves polycomb silencing. Mol Cell 2019;74:1138–47.
101. Wang T, Yu H, Hughes NW, Liu B, Kendirli A, Klein K, et al. Gene essentiality profiling reveals gene networks and synthetic lethal interactions with oncogenic Ras. Cell 2017;168:890–903.
102. Vu LP, Pickering BF, Cheng Y, Zaccara S, Nguyen D, Minuesa G, et al. The N6-methyladenosine (m6A)-forming enzyme METTL3 controls myeloid differentiation of normal hematopoietic and leukemia cells. Nat Med 2017;23: 1369–76.
103. Luo Z, Lin C, Shilatifard A. The super elongation complex (SEC) family in transcriptional control. Nat Rev Mol Cell Biol 2012;13:543–7.
104. Cancer Genome Atlas Research Network; Brat DJ, Verhaak RG, Aldape KD, Yung WK, Salama SR, et al. Comprehensive, integrative genomic analysis of diffuse lower-grade gliomas. N Engl J Med 2015;372:2481–98.
105. Mardis ER, Ding L, Dooling DJ, Larson DE, McLellan MD, Chen K, et al. Recurring mutations found by sequencing an acute myeloid leukemia genome. N Engl J Med 2009;361:1058–66.
106. Papaemmanuil E, Gerstung M, Bullinger L, Gaidzik VI, Paschka P, Roberts ND, et al. Genomic classification and prognosis in acute myeloid leukemia. N Engl J Med 2016;374:2209–21.
107. Qing Y, Dong L, Gao L, Li C, Li Y, Han L, et al. R-2-hydroxyglutarate attenuates aerobic glycolysis in leukemia by targeting the FTO/m(6)A/PFKP/LDHB axis. Mol Cell 2021;81:922–39.
108. Sundar SJ, Hsieh JK, Manjila S, Lathia JD, Sloan A. The role of cancer stem cells in glioblastoma. Neurosurg Focus 2014;37:E6.
109. Cui Q, Shi H, Ye P, Li L, Qu Q, Sun G, et al. m(6)A RNA methylation regulates the self-renewal and tumorigenesis of glioblastoma stem cells. Cell Rep 2017;18: 2622–34.
110. Xiao L, Li X, Mu Z, Zhou J, Zhou P, Xie C, et al. FTO inhibition enhances the antitumor effect of temozolomide by targeting MYC-miR-155/23a cluster-MXI1 feedback circuit in glioma. Cancer Res 2020;80:3945–58.
111. Zervos AS, Gyuris J, Brent R. Mxi1, a protein that specifically interacts with Max to bind Myc-Max recognition sites. Cell 1993;72:223–32.
112. Yamaki T, Suenaga Y, Iuchi T, Alagu J, Takatori A, Itami M, et al. Temozolomide suppresses MYC via activation of TAp63 to inhibit progression of human glioblastoma. Sci Rep 2013;3:1160.
113. Liu J, Ren D, Du Z, Wang H, Zhang H, Jin Y. m(6)A demethylase FTO facilitates tumor progression in lung squamous cell carcinoma by regulating MZF1 expression. Biochem Biophys Res Commun 2018;502: 456–64.
114. Ding Y, Qi N, Wang K, Huang Y, Liao J, Wang H, et al. FTO facilitates lung adenocarcinoma cell progression by activating cell migration through mRNA demethylation. Onco Targets Ther 2020;13:1461–70.
115. Tsai LH, Wu JY, Cheng YW, Chen CY, Sheu GT, Wu TC, et al. The MZF1/c-MYC axis mediates lung adenocarcinoma progression caused by wild-type lkb1 loss. Oncogene 2015;34:1641–9.
116. Li J, Han Y, Zhang H, Qian Z, Jia W, Gao Y, et al. The m6A demethylase FTO promotes the growth of lung cancer cells by regulating the m6A level of USP7 mRNA. Biochem Biophys Res Commun 2019;512:479–85.
117. Harbeck N, Penault-Llorca F, Cortes J, Gnant M, Houssami N, Poortmans P, et al. Breast cancer. Nat Rev Dis Primers 2019;5:66.
118. Niu Y, Lin Z, Wan A, Chen H, Liang H, Sun L, et al. RNA N6-methyladenosine demethylase FTO promotes breast tumor progression through inhibiting BNIP3. Mol Cancer 2019;18:46.
119. Xu Y, Ye S, Zhang N, Zheng S, Liu H, Zhou K, et al. The FTO/miR-181b-3p/ARL5B signaling pathway regulates cell migration and invasion in breast cancer. Cancer Commun 2020;40:484–500.
120. Dykes SS, Gray AL, Coleman DT, Saxena M, Stephens CA, Carroll JL, et al. The Arf-like GTPase Arl8b is essential for three-dimensional invasive growth of prostate cancer in vitro and xenograft formation and growth *in vivo*. Oncotarget 2016;7:31037–52.
121. Berulava T, Rahmann S, Rademacher K, Klein-Hitpass L, Horsthemke B. N6-adenosine methylation in MiRNAs. PLoS One 2015;10:e0118438.
122. Han D, Liu J, Chen C, Dong L, Liu Y, Chang R, et al. Anti-tumour immunity controlled through mRNA m(6)A methylation and YTHDF1 in dendritic cells. Nature 2019;566:270–4.
123. Lasman L, Krupalnik V, Viukov S, Mor N, Aguilera-Castrejon A, Schneir D, et al. Context-dependent functional compensation between Ythdf m6A reader proteins. Genes Dev 2020;34:1373–91.
124. Zaccara S, Jaffrey SR. A unified model for the function of YTHDF proteins in regulating m(6)A-modified mRNA. Cell 2020;181:1582–95.
125. Liu Y, Liang G, Xu H, Dong W, Dong Z, Qiu Z, et al. Tumors exploit FTO-mediated regulation of glycolytic metabolism to evade immune surveillance. Cell Metab 2021;33:1221–33.
126. Huang H, Wang Y, Kandpal M, Zhao G, Cardenas H, Ji Y, et al. FTO-dependent N (6)-methyladenosine modifications inhibit ovarian cancer stem cell self-renewal by blocking cAMP signaling. Cancer Res 2020;80:3200–14.
127. Li J, Zhu L, Shi Y, Liu J, Lin L, Chen X. m6A demethylase FTO promotes hepatocellular carcinoma tumorigenesis via mediating PKM2 demethylation. Am J Transl Res 2019;11:6084–92.
128. Sun D, Zhao T, Zhang Q, Wu M, Zhang Z. Fat mass and obesity-associated protein regulates lipogenesis via m(6) A modification in fatty acid synthase mRNA. Cell Biol Int 2021;45:334–44.
129. Mittenbuhler MJ, Saedler K, Nolte H, Kern L, Zhou J, Qian SB, et al. Hepatic FTO is dispensable for the regulation of metabolism but counteracts HCC development *in vivo*. Mol Metab 2020;42:101085.
130. Ma JZ, Yang F, Zhou CC, Liu F, Yuan JH, Wang F, et al. METTL14 suppresses the metastatic potential of hepatocellular carcinoma by modulating N(6) -methyladenosine-dependent primary MicroRNA processing. Hepatology 2017;65:529–43.
131. Rong ZX, Li Z, He JJ, Liu LY, Ren XX, Gao J, et al. Downregulation of fat mass and obesity associated (FTO) promotes the progression of intrahepatic cholangiocarcinoma. Front Oncol 2019;9:369.
132. Jeschke J, Collignon E, Al Wardi C, Krayem M, Bizet M, Jia Y, et al. Down-regulation of the FTO m6A RNA demethylase promotes EMT-mediated progression of epithelial tumors and sensitivity to Wnt inhibitors. Nat Cancer 2021;2: 611–28.
133. Chen B, Ye F, Yu L, Jia G, Huang X, Zhang X, et al. Development of cell-active N6-methyladenosine RNA demethylase FTO inhibitor. J Am Chem Soc 2012; 134:17963–71.
134. Islam MS, Leissing TM, Chowdhury R, Hopkinson RJ, Schofield CJ. 2-Oxoglutarate-dependent oxygenases. Annu Rev Biochem 2018;87:585–620.
135. Rose NR, McDonough MA, King ON, Kawamura A, Schofield CJ. Inhibition of 2-oxoglutarate dependent oxygenases. Chem Soc Rev 2011;40:4364–97.
136. Toh JDW, Sun L, Lau LZM, Tan J, Low JJA, Tang CWQ, et al. A strategy based on nucleotide specificity leads to a subfamily-selective and cell-active inhibitor of N(6)-methyladenosine demethylase FTO. Chem Sci 2015;6:112–22.

137. Huang Y, Yan J, Li Q, Li J, Gong S, Zhou H, et al. Meclofenamic acid selectively inhibits FTO demethylation of m6A over ALKBH5. Nucleic Acids Res 2015;43:373–84.
138. Huang Y, Su R, Sheng Y, Dong L, Dong Z, Xu H, et al. Small-molecule targeting of oncogenic FTO demethylase in acute myeloid leukemia. Cancer Cell 2019;35:677–91.
139. Huff S, Tiwari SK, Gonzalez GM, Wang Y, Rana TM. m(6)A-RNA demethylase FTO inhibitors impair self-renewal in glioblastoma stem cells. ACS Chem Biol 2021;16:324–33.
140. Su R, Dong L, Li Y, Gao M, Han L, Wunderlich M, et al. Targeting FTO suppresses cancer stem cell maintenance and immune evasion. Cancer Cell 2020;38:79–96.
141. Liu N, Pan T. Probing N 6-methyladenosine (m6A) RNA modification in total RNA with SCARLET. Methods Mol Biol 2016;1358:285–92.
142. Castellanos-Rubio A, Santin I, Olazagoitia-Garmendia A, Romero-Garmendia I, Jauregi-Miguel A, Legarda M, et al. A novel RT-QPCR-based assay for the relative quantification of residue specific m6A RNA methylation. Sci Rep 2019;9:4220.
143. Zhu Y, Shen J, Gao L, Feng Y. Estrogen promotes fat mass and obesity-associated protein nuclear localization and enhances endometrial cancer cell proliferation via the mTOR signaling pathway. Oncol Rep 2016;35:2391–7.
144. Song H, Wang Y, Wang R, Zhang X, Liu Y, Jia G, et al. SFPQ is an FTO-binding protein that facilitates the demethylation substrate preference. Cell Chem Biol 2020;27:283–91.
145. Weng H, Huang H, Wu H, Qin X, Zhao BS, Dong L, et al. METTL14 inhibits hematopoietic stem/progenitor differentiation and promotes leukemogenesis via mRNA m(6)A modification. Cell Stem Cell 2018;22:191–205.